MITSUBISHI ELECTRIC RESEARCH LABORATORIES
http://www.merl.com

Fully-Parallel Soft-Decision Cycle Slip Recovery

Koike-Akino, T.; Yoshida, T.; Parsons, K.; Millar, D.S.; Kojima, K.; Pajovic, M.

TR2017-023 March 2017

Abstract

We propose a parallel cycle slip recovery method employing soft-decision slipstate estimation at pilots. Through mutual information analysis, we show that the proposed method achieves 0.6 dB gain in the presence of frequent cycle slips and strong phase noise

Optical Fiber Communication Conference and Exposition and the National Fiber Optic Engineers Conference (OFC/NFOEC)

Fully-Parallel Soft-Decision Cycle Slip Recovery

Toshiaki Koike-Akino[1], Tsuyoshi Yoshida[2], Kieran Parsons[1], David S. Millar[1], Keisuke Kojima[1], Milutin Pajovic[1]

[1] *Mitsubishi Electric Research Labs. (MERL), 201 Broadway, Cambridge, MA 02139, USA.* *koike@merl.com*
[2] *Information Technology R&D Center, Mitsubishi Electric Corp., Ofuna, Kanagawa 247-8501, Japan*

Abstract: We propose a parallel cycle slip recovery method employing soft-decision slip-state estimation at pilots. Through mutual information analysis, we show that the proposed method achieves 0.6 dB gain in the presence of frequent cycle slips and strong phase noise.

OCIS codes: (060.4510) Optical communications, (060.1660) Coherent communications

1. Introduction

Phase noise, e.g., induced by laser linewidth [1] and fiber nonlinearity [2], has been one of major impairments in coherent optical communications. To tackle the phase noise impairments, blind carrier phase estimation (CPE) [3–7] has been adopted in various practical systems. Although pilot-aided CPE [8] and turbo CPE [9] may be able to achieve better performance, blind CPE based on Viterbi&Viterbi (V&V) method is often used in practice due to its hardware simplicity, in particular for low-order modulation schemes such as quadrature phase-shift keying (QPSK).

The V&V blind CPE has relatively large residual phase noise, and moreover it can cause frequent cycle slips [10–12] due to phase ambiguity. Beygi *et al.* [13] studied constellation design robust to the residual phase noise. Cao *et al.* [14] proposed a phase noise-aware log-likelihood ratio (LLR) calculation based on a Tikhonov model. An alternative LLR calculation method, employing linear or bilinear transform [15], was also investigated to improve robustness against residual phase noise. Cycle slip issues have been dealt with by turbo slip recovery [16], which uses a hidden Markov model of stochastic cycle slips. Zhang *et al.* [17] used pilots to mitigate cycle slips. Schmalen [18] proposed a new low-density parity-check (LDPC) code structure, which is robust to cycle slips.

In this paper, we propose a novel soft-decision cycle slip recovery method, which is suitable for parallel hardware implementation. The proposed method uses pilots to refine the LLR calculation by taking the residual phase noise and cycle slip probability into account. Through generalized mutual information (GMI) [19] analysis, we show that up to 0.6 dB gain can be achieved by the proposed method in the presence of the cycle slip probability higher than 10^{-4}.

2. Cycle Slip and Residual Phase Noise

Fig. 1 shows a schematic of the blind CPE, followed by the soft-decision cycle slip recovery. As the proposed method uses the statistical information of slip rate p_s and the residual phase noise variance σ_e^2 of the blind CPE, we first investigate the slip probability and the residual phase noise in the conventional blind CPE. We consider QPSK transmission and the 4-th power CPE method having an averaging filter window of length $2L+1$.

In Fig. 2, we show the cycle slip probability p_s and mean-square error (MSE) σ_e^2 of phase estimation for the blind CPE with $L = 31$ under additive white Gaussian noise (AWGN) channels in the presence of Wiener process phase noise, whose variance is $\sigma_\mathrm{p}^2 = 2\pi\Delta\nu T_\mathrm{s} \in \{10^{-2}, 10^{-3}, 10^{-4}, 10^{-5}\}$. Here, $\Delta\nu$ and T_s are an effective linewidth and symbol duration, respectively. For example, $\sigma_\mathrm{p}^2 = 10^{-4}$ corresponds to a laser linewidth of 477 kHz for 30 GBd.

From Fig. 2, we can observe that frequent slip rates $p_\mathrm{s} \geq 10^{-4}$ can occur in low signal-to-noise ratio (SNR) regimes, even for small phase noise variance of $\sigma_\mathrm{p}^2 \leq 10^{-4}$. This is because the cycle slip is dominated by the noise enhancement [10] even without phase noise. Such noise enhancement can be reduced by increasing the averaging filter window size, as shown in Fig. 3, where the slip rate and MSE curves are present for the half window lengths of $L \in \{31, 63, 127\}$ at $\sigma_\mathrm{p}^2 = 10^{-4}$. Although longer window size can reduce the slip probability, the MSE does not improve much. Moreover, we are often unable to use a large window size in practical hardware because high-speed parallel processing becomes more difficult to implement for longer averaging windows.

Consequently, a major challenge arises in the cases when filter length is constrained and the SNR is low. Therefore, this paper focuses on a practically reasonable filter with half window length $L = 31$ and a target spectral efficiency of 1.0–1.5 b/s/Hz/pol, whose required SNR in Shannon limit ranges from 0 dB to 3.5 dB in AWGN channels when no phase noise is present.

3. Pilot-Aided Soft-Decision Cycle Slip Recovery

The signal after the blind CPE is modeled as $y_n = x_n \exp\{\mathrm{j}(\theta_n + \frac{\pi}{2}s_n)\} + w_n$, where y_n is the symbol feeding into the demodulator, x_n is the transmitted QPSK symbol, θ_n is the residual phase noise, which follows the Gaussian distribution $\mathbb{N}(0, \sigma_e^2)$, and w_n is an additive noise following the circular-symmetric complex Gaussian distribution $\mathbb{CN}(0, \sigma^2)$, at the n-th symbol. Here, s_n represents the slip state due to the phase ambiguity of the blind CPE. To account for the residual phase noise, we use a moment-matching method as $\exp(\mathrm{j}\theta_n) \in \mathbb{CN}(\mu, 1-\mu^2)$ with $\mu = \exp(-\sigma_e^2/2)$, and the LLR values calculated at the demodulator in Fig. 1 are first scaled by $\mu^2\sigma^2/(\sigma^2 + 1 - \mu^2)$.

The LLR is further modified by using pilot-aided soft-decision recovery depicted in Fig. 4, where we consider the slip states s_n as a Markov process. Using the soft-decision slip state probability $\Pr(s_n|y_n)$ given by LLR values at M nearest pilots, the LLR at data symbols are refined in parallel. Since the probability that the slip state s_{n+m} stays the same state s_n decays exponentially as a function of m, we use weighted LLRs from M pilots by the m-th power of state transition matrix $\boldsymbol{T}$. For the Markov process with a slip rate p_s, the state transition matrix can be pre-computed as $\boldsymbol{T}[q] = \mathscr{T}[(1-q)^2, q(1-q), q^2, q(1-q)]$, where $\mathscr{T}[\cdot]$ denotes the Toeplitz matrix and $q = 1 - \sqrt{1-p_\mathrm{s}}$. Using the Toeplitz property, $\boldsymbol{T}^m[q]$ is easily calculated by $\boldsymbol{T}[q']$ with $q' = (1-(1-2q)^m)/2 \simeq mq$. This LLR modification can be carried out in a fully parallel manner because no decision feedback or sequential update is required.

4. Performance Results

Here, we analyze the GMI performance of the proposed soft-decision cycle slip recovery for the 4-th power CPE with $L = 31$. Fig. 5 shows the GMI curves at different phase noise variance $\sigma_\mathrm{p}^2 \in \{10^{-3}, 10^{-4}, 10^{-5}\}$. We use two adjacent pilots ($M = 2$) to make an estimate of slip states, and a pilot insertion interval of $N = 100$ symbols. Note that the GMI penalty from the Shannon limit is significant because the residual phase noise and slip rates are non-negligible as shown in Fig. 2. Nevertheless, one can see that the proposed soft-decision slip recovery achieves 0.5–0.8 dB gain at a target spectral efficiency of 1.0–1.5 b/s/Hz/pol, in the presence of large phase noise $\sigma_\mathrm{p}^2 = 10^{-3}$.

Fig. 6 shows the impact of pilot insertion interval N. We can see that short intervals improve the tolerance against cycle slips in low SNR regimes, whereas longer intervals can improve the GMI in higher SNRs due to lower overhead. When we compare the soft- and hard-decision recovery at a best pilot insertion interval N, 0.3–0.6 dB gain can be obtained by the proposed scheme for the target spectral efficiency. Although more gain can be seen in a spectral efficiency lower than 1.0 b/s/Hz/pol, we shall use lower-order modulation with higher code rates for those SNR regimes.

5. Conclusions

We have proposed a new soft-decision cycle slip recovery method which is suitable for parallel hardware implementation. Using LLR modification by adjacent pilots, we can improve the tolerance against cycle slips. Through GMI analysis, we have shown that the proposed scheme outperforms the hard-decision counterpart by up to 0.5 dB in the presence of frequent cycle slips, caused by the blind CPE with a short window.

References

1. K. Kikuchi, "Characterization of semiconductor-laser phase noise and estimation of bit-error rate performance with low-speed offline digital coherent receivers," *OpEx* **20** 5 (2012), pp. 5291–5302.
2. A. P. T. Lau, J. M. Kahn, "Signal design and detection in presence of nonlinear phase noise," *JLT* **25** 10 (2007), pp. 3008–3016.
3. E. Ip, J. M. Kahn, "Feedforward carrier recovery for coherent optical communications," *JLT* **25** 9 (2007), pp. 2675–2692.
4. M. G. Taylor, "Phase estimation methods for optical coherent detection using digital signal processing," *JLT* **27** 7 (2009), pp. 901–914.
5. F. A. Garcia, D. A. Mello, H. Waldman, "Feedforward carrier recovery for polarization demultiplexed signals with unequal signal to noise ratios," *OpEx* **17** 10 (2009), pp. 7958–7969.
6. M. Kuschnerov et al., "Joint-polarization carrier phase estimation for XPM-limited coherent polarization-multiplexed QPSK transmission with OOK-neighbors," in *ECOC* (2008), paper Mo4.D.2.
7. Y. Gao, A. P. T. Lau, S. Yan, C. Lu, "Low-complexity and phase noise tolerant carrier phase estimation for dual-polarization 16-QAM systems," *OpEx* **19** 22 (2011), pp. 21717–21729.
8. M. Pajovic et al., "Experimental demonstration of multi-pilot aided carrier phase estimation for DP-64QAM and DP-256QAM," in *ECOC* (2015), paper Mo.4.3.3.
9. X. Wu, H. Xiang, "Iterative carrier phase recovery methods in turbo receivers," *IEEE COMLET* **9** 8 (2005), pp. 735–737.
10. E. Ibragimov, B. Zhang, T. J. Schmidt, C. Malouin, N. Fediakine, H. Jiang, "Cycle slip probability in 100G PM-QPSK systems," in *OFC* (2010), paper OWE2.
11. C. R. S. Fludger, D. Nuss, T. Kupfer, "Cycle-slips in 100G DP-QPSK transmission systems," in *OFC* (2012), paper OTu2.G1.
12. T. Pfau, J. Lee, N. Kaneda, "Parity check encoded QPSK for rate adaptation in coherent DSP-based receivers," *IEEE PLT* **26** 15 (2014), pp. 1538–1541.
13. L. Beygi, E. Agrell, M. Karlsson, "Optimization of 16-point ring constellations in the presence of nonlinear phase noise," in *OFC* (2011), paper OThO4.
14. S. Cao et al., "Pilot-tone assisted log-likelihood ratio for LDPC coded CO-OFDM system," *IEEE PTL* **26** 15 (2014), pp. 1577–1580.
15. T. Koike-Akino et al., "Phase noise-robust LLR calculation with linear/bilinear transform for LDPC-coded coherent communications," in *CLEO* (2015), paper SW1M-3.
16. T. Koike-Akino et al., "Cycle slip-mitigating turbo demodulation in LDPC-coded coherent optical communications," in *OFC* (2014), paper M3A.3.
17. H. Zhang, Y. Cai, D. G. Foursa, A. N. Pilipetskii, "Cycle slip mitigation in POLMUX-QPSK modulation," in *OFC* (2011), paper OMJ7.
18. L. Schmalen, "A low-complexity LDPC coding scheme for channels with phase slips," *JLT* **33** 7 (2015), pp. 1319–1325.
19. A. Alvarado, E. Agrell, D. Lavery, R. Maher, P. Bayvel, "Replacing the soft FEC limit paradigm in the design of optical communication systems," *JLT* **33** 20 (2015), pp. 4338–4352.

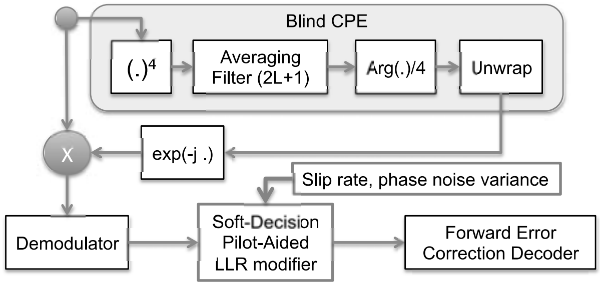

Fig. 1: Blind CPE and soft-decision cycle slip recovery.

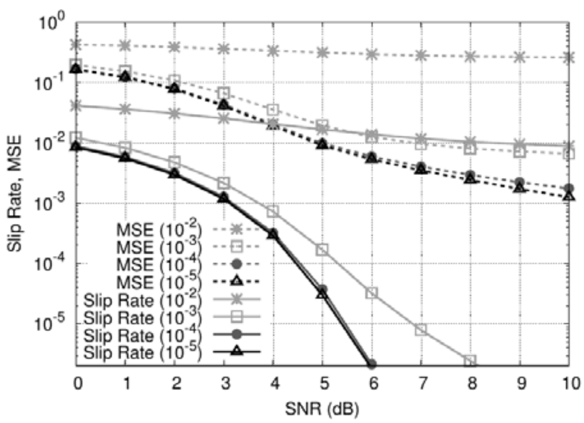

Fig. 2: Slip rate and MSE of 4-th power CPE with $L=31$ for QPSK at $\sigma_{\mathrm{p}}^2 = 2\pi\Delta\nu T_{\mathrm{s}} \in \{10^{-2}, 10^{-3}, 10^{-4}, 10^{-5}\}$.

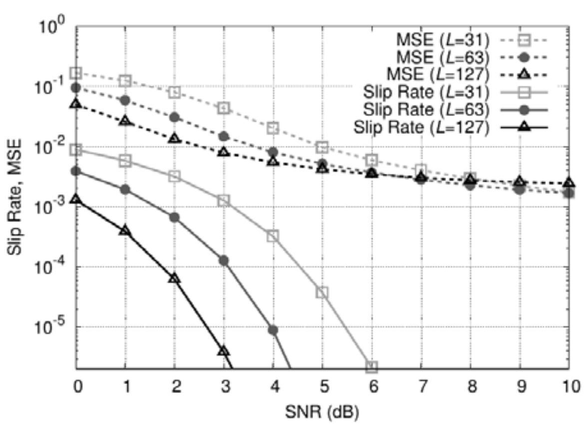

Fig. 3: Slip rate and MSE of 4-th power CPE with $L \in \{31, 63, 127\}$ for QPSK at $\sigma_{\mathrm{p}}^2 = 10^{-4}$.

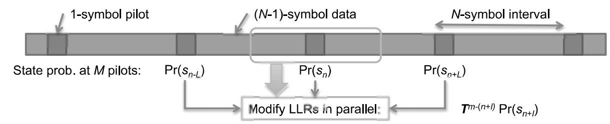

Fig. 4: Fully parallel M-pilot cycle slip recovery.

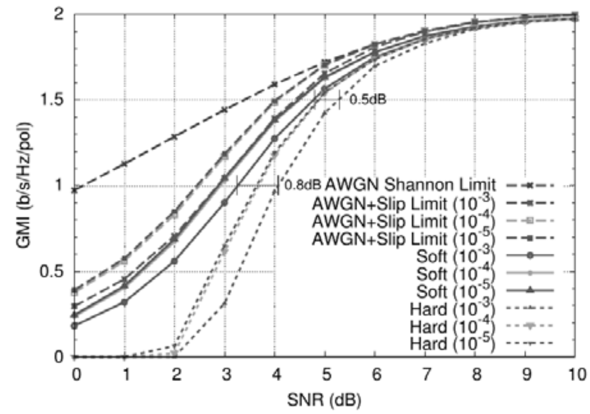

Fig. 5: GMI of 2-pilot soft- and hard-decision slip recovery with pilot insertion interval $N = 100$ for 4-th power CPE with $L = 31$ and QPSK at $\sigma_{\mathrm{p}}^2 \in \{10^{-3}, 10^{-4}, 10^{-5}\}$.

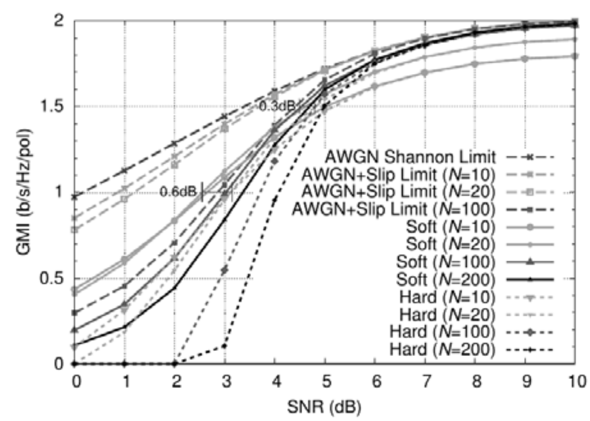

Fig. 6: GMI of 3-pilot soft- and hard-decision slip recovery with different pilot insertion interval $N \in \{10, 20, 100, 200\}$ for $L = 31$ and QPSK at $\sigma_{\mathrm{p}}^2 = 10^{-3}$.